The spectral analysis and mode structure of ultrabroad InAs/InAlGaAs quantum dash laser

C. L. Tan[a], Y. H. Ding[a], C. E. Dimas[a], H. S. Djie[b], Y. Wang[c], V. Hongpinyo[a], C. Chen[a], B. S. Ooi[a]
[a]Center for Optical Technologies and Department of Electrical and Computer Engineering, Lehigh University, 7 Asa Drive, Bethlehem, PA, USA 18015;
[b]JDS Uniphase Corporation, San Jose, CA, USA 95134;
[c]OptiComp Corporation, Zephyr Cove, NV, USA 89448

ABSTRACT

We demonstrate the widened broadband emission of self-assembled quantum dash laser using impurity-free vacancy induced disordering (IFVD) technique. The 100 nm blueshifted lasers exhibit higher internal quantum efficiency and lower threshold current densities than the as-grown devices. The laser emission from multiple groups of quantum-dash (Qdash) families convoluted with multiple orders of subband energy levels within a single Qdash ensemble is experimentally observed. However, the suppression of laser emission in short wavelength and the progressive redshift of peak emission with injection current from devices with short cavity length occur. These effects have been attributed to the nonequilibrium carrier distribution and energy exchange among different sizes of Qdash ensembles. In addition, we perform the far-field lateral mode measurements from the fabricated as-grown Qdash laser. The analysis of mode patterns indicate that Qdash lasers exhibit gradual broadening of beam divergence (FWHM of 3.4° to 10.8°) with increasing injection current. However, these beam divergence angles are still narrower than the quantum well (QW) laser (FWHM ~13º) at an injection up to 2.5 x J_{th}. Qdash laser exhibits an improved output beam quality, therefore reduced filamentation, as compared to the QW laser, owing to the inherent characteristics from quantum-dot (Qdot) laser, where injected carriers are confined by the lateral energy barriers as Qdots are disconnected laterally and are cladded by larger bandgap materials. Our results imply a highly attractive wavelength trimming method, well suited for improved performance, and monolithic Qdash integration of optoelectronics components.

Keywords: Semiconductor laser, self-assembled quantum dash, quasi-supercontinuum, optical gain broadening, broadband laser, inhomogeneous broadening, intermixing, far-field pattern, optical beam divergence.

1. INTRODUCTION

Self-assembled quantum-dot (Qdot)/quantum-dash (Qdash) semiconductor nanostructures have attracted considerable interest in the fabrication of semiconductor lasers and optical amplifiers due to the unprecedented potential offered by the three-dimensional energy levels quantification that lead to vastly improved optoelectronic characteristics as compared to conventional quantum-well (QW) structures and bulk materials [1-3]. In particular, self-assembled Qdot lasers have been shown to emit unique lasing spectral characteristics, where the laser emission spectra are broadened with modulated non-lasing spectral regions and the number of lasing modes increases above threshold [4]. This behavior has been attributed to the carrier localization in noninteracting or spatially isolated dot ensembles and a resultant inhomogeneously broadened gain spectrum in dispersive dots. On the other hand, an extraordinary wideband lasing coverage of 50 nm, in the absence of modulated non-lasing spectral regions, but only at low temperature (60 K) from Qdot laser has been reported [5]. This phenomenon is attributed to the nonequilibrium carrier distribution among self-assembled Qdot with different sizes and compositions due to the longer carrier emission time [6]. The most recent study reveals that a low-ripple (<3 dB) wideband lasing coverage of ~40 nm from Qdot lasers can be achieved at room temperature without any sign of non-lasing spectral regions at ~1160 nm center wavelength [7, 8]. More so, the characteristic of broadband emission from Qdot laser [7, 8] at high temperature such as room temperature (20 ºC) with the proposed role of optical gain broadening [9] is also inherent in Qdash lasers [10-12].

These interesting features of broad interband lasing actions from self-organized, spatially-isolated semiconductor nanostructure technology can be widely applied in optical telecommunications, various sensors detecting

Quantum Dots, Particles, and Nanoclusters VI,
edited by Kurt G. Eyink, Frank Szmulowicz, Diana L. Huffaker, Proc. of SPIE Vol. 7224,
72240S · © 2009 SPIE · CCC code: 0277-786X/09/$18 · doi: 10.1117/12.808567

chemical agents, atmospheric or planetary gases, high-precision optical metrology and spectroscopy, and biomedical imaging [10]. In addition, it is natural to expect that narrow pulses can be generated by locking the phases of modes in this quasi-supercontinuum interband laser spectrum under mode-locked operation [13] due to the fast carrier dynamics and the broad optical gain bandwidth [2]. Furthermore, the high power emission capability of ~1 W per device from these ultrabroadband Qdash lasers at room temperature can be potentially employed as a high efficiency resonant pumping source [14] for eye-safe Er-doped amplifiers and solid-state lasers.

However, broad-area edge-emitters tend to exhibit self stabilized nonlinear modes and thus the issue of self-focusing will induce high-brightness unstable filaments, which destroys the spatial coherence of the beam and can lead to catastrophic optical damage (COD) at the laser facet [15]. Several methods to overcome this problem have been proposed and applied to produce narrow beam divergence to reduce the complexity and cost of an optical system. However, the lack of studies on the effect of different active gain mediums on the spatial coherence properties may hinder a better understanding of the nature of far-field pattern formation from semiconductor lasers. Numerical simulations indicate that filamentation for broad-area lasers with a stripe width > 50 μm occurs if α exceeds 0.5 [16]. Recent studies show that generally QW exhibits the largest α, followed by Qdash and Qdot [17, 18].

In this work, we demonstrate the widened broadband emission of Qdash laser using IFVD technique. The intermixed lasers exhibit higher internal quantum efficiency and lower threshold current densities as compared to the as-grown devices. The laser emission from multiple groups of Qdash families convoluted with multiple orders of subband-energy levels within a Qdash ensemble indicates nonequilibrium carrier distribution and localized photon reabsoprtion. Apart from the spectral analysis, we perform the measurements and analysis of far field pattern from lasers with two different geometries of active gain mediums such as InGaAs/InGaAsP QW and InA/InAlGaAs Qdash semiconductor lasers. The QW and Qdash lasers give light emission at long wavelength of ~1.55 μm and ~1.64 μm, respectively. Our results imply a highly attractive wavelength trimming method, well suited for improved performance, and monolithic Qdash integration of optoelectronics components.

2. EXPERIMENTS

The lattice-matched InGaAs/InGaAsP QW laser structure in this study was grown by metal organic chemical vapor deposition (MOCVD) on a Si-doped n-InP substrate. The structure is based on a standard separate confinement heterostructure (SCH) with two sets of multiple QWs. The upper SCH layers and the lower SCH layers are each 155nm-thick film of InGaAsP layer and an inner 600nm-thick film of doped InGaAsP. The undoped active region consists of two sets of multiple QWs with matching photoluminescence peaks: five 10nm $In_{0.446}Ga_{0.554}As$ wells with 20nm GaInAsP barriers and 6 (underlying) lattice matched 5.5nm $In_{0.47}Ga_{0.53}As$ wells with 12 nm GaInAsP barriers. In InAs/InAlGaAs Qdash laser, the epitaxial structure was grown by molecular beam epitaxy (MBE) on (100) oriented InP substrate. The active region consists of four sheets of 5 monolayer (ML) InAs dashes, each embedded within a 7.6 nm thick compressively strained $In_{0.64}Ga_{0.16}Al_{0.2}As$ QW and a 30 nm thick tensile strained $In_{0.50}Ga_{0.32}Al_{0.18}As$ barrier. The details of this structure can be found elsewhere [19, 20].

We performed the dielectric cap annealing technique to induce selective intermixing using 475 nm thick SiO_2 layer as a group-III vacancy source deposited using plasma enhanced chemical vapor deposition technique. During the annealing, the SiO_2 cap will enhance the preferential atomic outdiffusion hence enhancing the group-III atomic interdiffusion in the Qdash active region resulting in the effective bandgap modification of Qdash material [19]. The dielectric cap also serves to protect the surface quality during annealing from the thermal induced decomposition. Following the dielectric cap removal, state-filling PL spectroscopy using a 980 nm diode laser as an excitation source was performed at 77 K to assess the bandgap modification from the interdiffusion effect on the laser structure. The IFVD process is performed by annealing the SiO_2 capped sample in nitrogen ambient for one minute in a rapid thermal processor (RTP). At the temperature of 750ºC, the PL peak shifts towards a shorter wavelength emission while the linewidth is the broadest [12]. Further increase in annealing temperature initiates more intermixing, and therefore improves the uniformity in shape, size and composition of Qdash leading to reduction in PL linewidth [19]. The result points out the linewidth broadening at intermediate stage of intermixing due to non-uniform interdiffusion, which will be further exploited to broaden the Qdash laser emission [12].

Broad area lasers with 50 μm wide oxide stripes are then fabricated from both the as-grown and intermixed Qdash samples with SiO_2 capped layer under annealing temperature of 750 ºC. In order to maximize the gain [3], the optical cavity of the laser is aligned along the [011] orientation and is perpendicular to the dash direction. Similar broad area lasers are fabricated as well from QW samples. Current injection was performed to the non-facet-coated Qdash lasers under pulsed operation at 0.2% duty cycle with a 2 μs pulse width. The far-field patterns of both as-grown Qdash and QW lasers are then measured by using a InGaAs photodetector.

3. RESULTS AND DISCUSSION

3.1 Optical properties of Qdash material

Carriers localized in different dots/dashes, resulting in a system without a global Fermi function and exhibiting an inhomogeneously broadened gain spectrum, have shown an interesting phenomenon of lasing spectra [4, 7, 9, 21]. This unique feature of dot/dash can be well studied from the evolution of state-filling spectroscopy from both as-grown and intermixed Qdash structures at 77 K under different excitation power densities, as shown in Figure 1 and its inset. At low excitation below 3 W/cm^2, the ground state emissions of 1.57 μm and 1.50 μm are dominant in the as-grown and the intermixed samples, respectively. The PL spectra are gradually broadened in both samples with increasing optical excitation densities. An increase in the excitation power density leads to the filling of lower-energy states, allowing recombination from higher energy levels of Qdash structure. Under the same excitation density, the PL linewidth of intermixed sample is wider than the as-grown sample. At the power excitation density of 1500 W/cm^2, the PL linewidth increases by 11 nm (from 94 nm to 111 nm) after intermixing process. The phenomenon of carrier localization in Qdash becomes more evident when the intermixed sample shows a larger variation of full-width-half-maximum (ΔFWHM up to 47 nm) than the as-grown sample (ΔFWHM up to 18 nm) under various power excitation densities relative to the FWHM obtained at the optical excitation of 3 W/cm^2 [12].

These enormously large broadening of the PL spectra from both as-grown and intermixed samples is attributed to the contribution of multiple transition states [7] or large inhomogeneous broadening of the non-interacting Qdash ensembles [12, 22]. This observation is also clearly different from that of both conventional QW [23] and Qdot structures [19]. The IFVD technique is generally known to improve the size homogeneity of a highly inhomogeneous semiconductor nanostructure system and thus will contribute to smaller variation in energy transition after intermixing. For instance, at the power excitation density of 1500 W/cm^2, the PL linewidth decreases by 6 nm (from 94 nm to 88 nm)

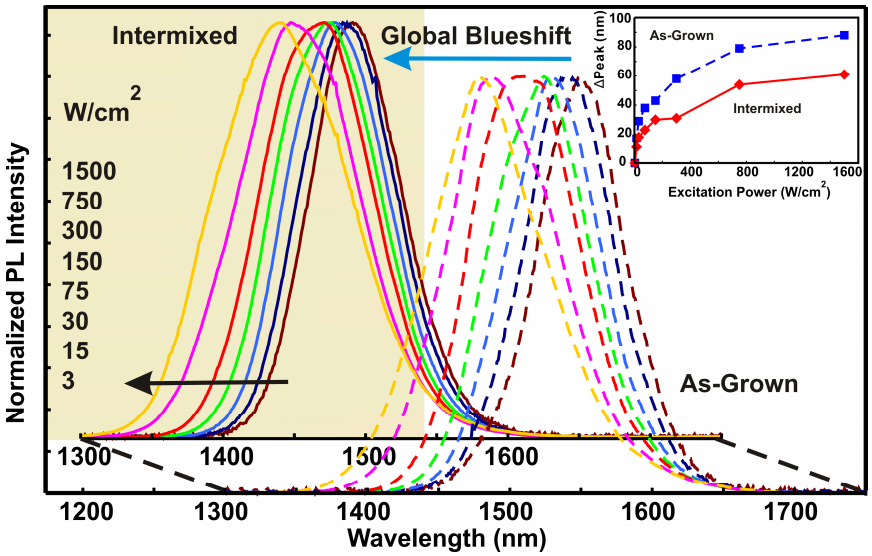

Fig. 1. The PL spectra of both as-grown and intermixed Qdash samples, with varying optical pumping levels, show global blueshift after intermixing. The inset shows the corresponding changes of PL peak wavelength as compared to those obtained under optical excitation of 3 W/cm^2.

after the IFVD process is performed by annealing the SiO_2 capped sample at 750ºC for two minutes [24]. However, the opposite observations in the Qdash, i.e. larger PL linewidth after intermediate intermixing, suggests the presence of different interdiffusion rates at a given intermixing degree in the Qdash nanostructures as a consequence of wide variation in surface to volume ratio in Qdash ensembles. The presence of more non-interacting Qdash with wider distribution of energy levels will contribute to radiative recombination emission over larger wavelength coverage and thus a larger FWHM in PL spectra. In other words, carrier localization is more prominent in an isolated Qdash, which affects the optical properties of these material systems. Nevertheless, both intermixed and as-grown Qdash samples showing saturation of ΔFWHM at excitation power over 400 W/cm^2 indicates that large degeneracy levels in highly confined energy states of Qdash is still preserved as can be seen in Qdot nanostructures [25].

The nearly symmetric Qdash PL spectra in Figure 1 are broadened with increasing optical excitation densities towards the shorter transition wavelength. The continuous blue-shift of the PL peak wavelength up to 88 nm in the as-grown sample and 61 nm in the intermixed sample at the optical excitation density of 1500 W/cm^2, relative to those obtained at the excitation of 3 W/cm^2, are shown in the inset of Figure 1. The large degree of blue-shift observed from sample excited under high density excitation is reasonably ascribed to the postulation of continuum states [22] in the Qdash nanostructures, although spectral widening at a shorter wavelength is expected in an inhomogeneous Qdash structure [25]. Continuum states serve as an effective medium for exciton scattering. The wide distribution of energy levels due to the nature of Qdash inhomogeneous (FWHM of 76 nm from PL measurement of as-grown sample at low excitation of 3 W/cm^2) will further serve as radiative recombination states or "sink" for the scattered excitons from the dense continuum states. Consequently, quasi-supercontinuum lasing spectra of the diode laser fabricated from these samples will be observed. However, smaller blue-shift of PL peak wavelength in the intermixed sample, as depicted in the inset of Figure 1, indicates that IFVD enhances the Qdash inhomogeneity more so in larger sizes of Qdashes, which emit at longer wavelengths [12]. Assuming a uniform injection of group-III vacancies from the surface during the IFVD process, the interdiffusion in the vertical direction will affect the dash height more than other directions [24, 26]. At an intermediate stage of intermixing, the thick dash family, where the quantized energy level located closer to the conduction band minima, will experience a larger degree of intermixing as the effective height or thickness of the dash decreases [12]. In addition, the local effective concentration for the thick dash family is higher than the thin dashes. Under uniform annealing temperature, the thick Qdash family that has larger interdiffusion length will yield larger degree of intermixing. As a result, largest degree of wavelength blue-shift (~65 nm) is observed at low excitation of 3 W/cm^2 (dominant emission from thick dashes) as compared to the smaller wavelength blue-shift (~38 nm) at high excitation of 1500 W/cm^2 (dominant emission from thin dashes).

3.2 Broad area laser characterization

Spectral widening is apparent as the bias increases [11, 12]. The localized active region of the device can be treated as a large number of Qdot or Qdash, which can be further treated as a broad distribution of discrete energy levels [5]. This is owed to the inhomogeneous broadening nature of Qdash ensembles and the dash variation from different dash stacks. The light-current (*L-I*) curve of the short cavity Qdash laser (L = 300μm) yields J_{th} and slope efficiency of 2.3 kA/cm^2 and 0.46 W/A, respectively, as depicted in the inset of Figure 2. Measuring the temperature dependent J_{th} over a range of 10-50 ºC, reveals the temperature characteristic (T_o) of 41.3 K.

The shorter cavity laser exhibits the progressive appearance of short wavelength emission line within a range of increasing injection level. Furthermore, the *L-I* curve of the short cavity laser shows kinks. The jagged *L-I* curve below ~3 x J_{th} implies that the lasing actions from different confined energy levels are not stable due to the occurrence of energy exchange between short and long wavelength lasing modes [25], as can be seen in the peak lasing line of Figure 2. In addition, the observation of kink in the *L-I* curve for device tested at low temperature might also be a result of mode competition in the gain-guided, broad area cavity devices. The calculated Fabry-Perot mode spacing of ~1.1 nm is well resolved in the measurement across the lasing wavelength span at low injection before a quasi-supercontinuum lasing is achieved. Subsequent injections contribute to the stimulated emission from longer wavelength or lower order subband energies while suppressing higher order subbands as shown in Figure 2. This Qdash laser behavior is fundamentally different from the experimental observation from Qdot lasers with short cavity length, where the gain of lower subband is too small to compensate for the total loss, and lasing proceeds via the higher order subbands [27, 28]. In short-cavity Qdash laser, the initial lasing peak at shorter wavelength (~1525 nm) is dominantly emitted from different groups of smaller size Qdash ensembles instead of higher order subbands of Qdash. Hence, the significant difference of ~11 meV as compared to the dominant lasing peak of ~1545 nm at high injection will contribute to photon reabsorption by larger

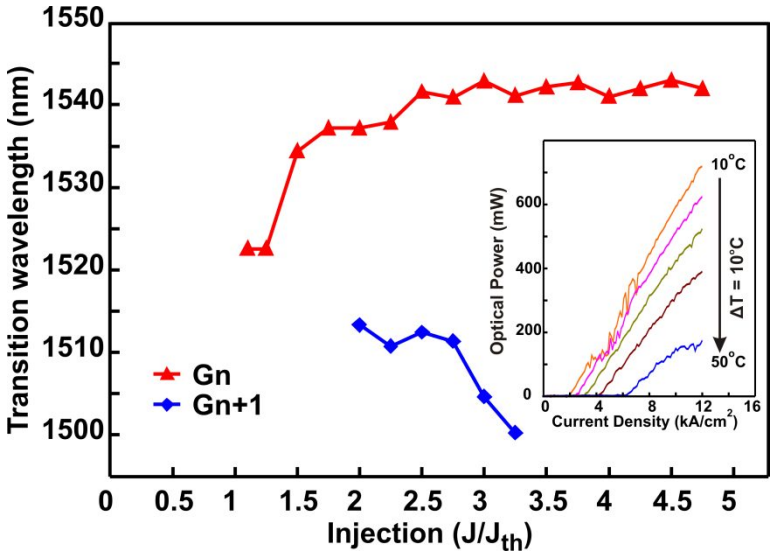

Fig. 2. The progressive change of lasing peak emission from different Qdash ensembles above threshold condition is shown from the 50 x 300 μm^2 broad area Qdash laser. The inset shows the corresponding *L-I* characteristics of the laser at different temperatures. Up to ~450 mW total output power (from both facets) has been measured at J = 4.0 x J_{th} at 20ºC.

size Qdash ensembles and seize the lasing actions at shorter wavelength. Regardless, a smooth *L-I* curve at the injection above 3 x J_{th} due to the only dominant lasing modes at long wavelength demonstrates the high modal gain of the Qdash active core [2]. These observations indicate that carriers are easily overflows to higher order subbands because of the large cavity loss and the small optical gain [5] at moderate injection. At high injection, carrier emission time becomes shorter, when equilibrium carrier distribution is reached and lasing from multiple Qdash ensembles is seized [6].

Distinctive lasing lines are observed from different cavity Qdash lasers at the near-threshold injection of J = 1.1 x J_{th}. The similarity of lasing wavelength from devices with different cavity lengths show promises that the Qdash structures have high modal gain characteristics [2]. However, the Qdash laser with increasing cavity length shows progressive red-shift (total of ~20 nm up to L = 1000 μm) of peak emission, as depicted in Figure 3 (a). At an injection

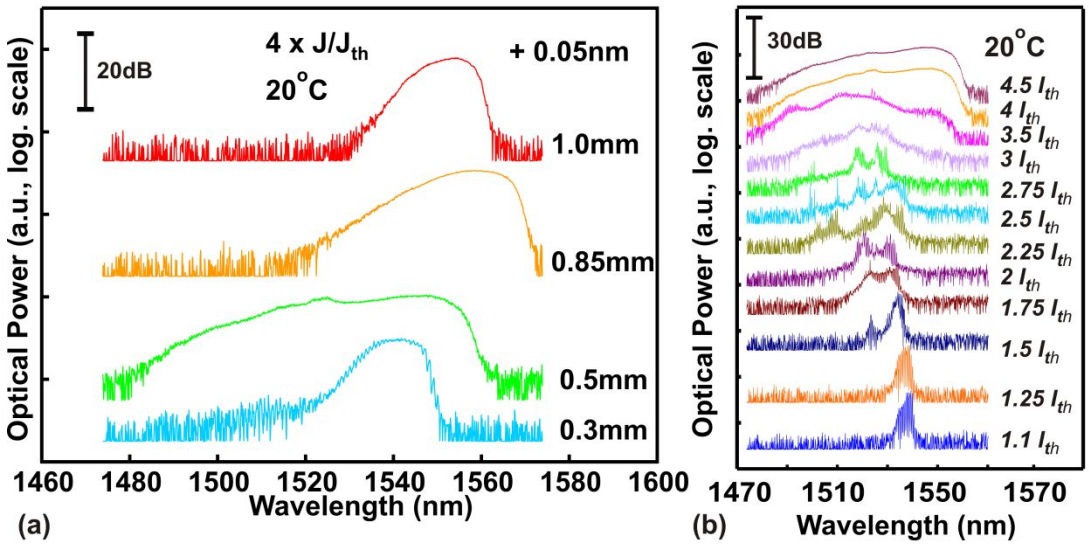

Fig. 3. The effect of cavity dependent on supercontinuum broadband emission from Qdash laser at the injection of J = 4 x J_{th}. (a) *L-I* characteristics of the 50 x 500 μm^2 broad area Qdash laser at different temperatures. Up to ~1 W total output power has been measured at J = 5.5 x J_{th} at 20ºC before showing sign of thermal roll-off. (b) The lasing spectra above threshold condition that are acquired by an optical spectrum analyzer with wavelength resolution of 0.05 nm.

of $J = 4$ x J_{th}, a continuous lasing spectra can be achieved from Qdash lasers with different cavities. This may be ascribed to the wide distribution of energy levels because of highly inhomogeneous broadening and photon reabsorption among Qdash families. At the intermediate injection of $J = 2.25$ x J_{th}, simultaneous two-state laser emission, which is attributed to two groups of Qdash ensembles as mentioned previously, is noticed from short cavity Qdash lasers. On the other hand, a broad linewidth laser emission from a single dominant wavelength is observed in longer cavity Qdash lasers of 850 μm and 1000 μm. As a result, a quasi-supercontinuum broad laser emission could be achieved at high injection, as shown in Figure 3(b). An ultrabroad quasi-supercontinuum lasing coverage from Qdash devices with $L = 500$μm [12] results from emission in different orders of energy subbands and different groups of Qdash ensembles. Bangap-tuned broad area lasers with optimum cavity length ($L = 500$ μm) that gives largest quasi-supercontinuum coverage of lasing emission, as presented in Figure 3, are fabricated. The *L-I* curve of the Qdash laser yields an improved J_{th} and slope efficiency of 2.1 kA/cm^2 and 0.423 W/A as compared to that of as-grown laser with 2.6 kA/cm^2 and 0.165 W/A, respectively [11]. The *L-I* curve of the intermixed laser shows kinks, which is similar to that of short cavity $L = 300$ μm Qdash lasers. The energy-state-hopping instead of mode-hopping occurs due to the wide distribution of the energy levels across the highly inhomogeneous Qdash active medium, as derived from the PL results from Figure 1. In spite of that, a smooth *L-I* curve above 6 kA/cm^2 yields a total high power of ~1 W per device at room temperature before any sign of thermal roll-over. This shows that injection above 6 kA/cm^2 provides enough carriers for population inversion in all the available or possible radiative recombination energy states and thus the energy-state-hopping is absent.

3.3 Far-field pattern measurement

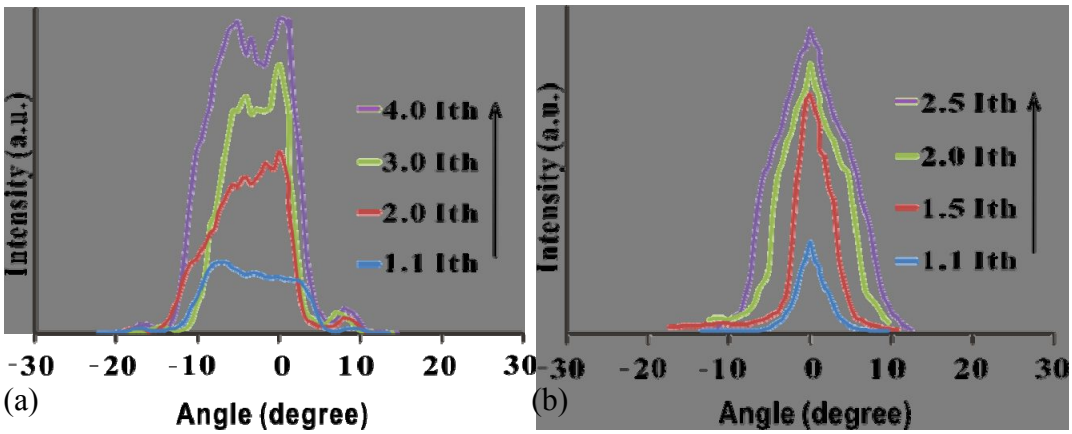

Fig. 4. (a) Far field profiles of the 50-μm-wide gain-guided QW broad area laser with a cavity length of 0.5 mm at different current injections. (b) Far field profiles of the 50-μm-wide gain-guided Qdash broad area laser with a cavity length of 0.5 mm at different current injections.

The threshold current densities of both as-grown InGaAs/InGaAsP QW and InAs/InAlGaAs Qdash lasers are 1.5 kA/cm^2 and 4 kA/cm^2, respectively. Figure 4 shows the far-field profiles of the lasers at different current injections. The measurements are done in pulsed-current injection amplitude coupling of the semiconductor medium that diffuses any local optical buildup and prevents the formation of filaments [29]. Although the comparison may not be fair as Qdash laser is injected up to only 2.5 x I_{th} but not 4 x I_{th}, filamentation is clearly shown at injection as low as 2 x I_{th}.

The far-field patterns illustrated in the figures are measured with the resolution of 0.5º step. The far-field profile of QW lasers in Figure 4(a) shows that high nonuniformity of the lowest order supermode present at even low injection (< 2 x J_{th}) and thus carriers are unevenly depleted when this mode is excited. At higher injection (> 2 x J_{th}), gain saturation or spatial hole burning in carrier concentration is expected to occur in semiconductor laser [30]. More and more higher order lateral modes are excited as the power level goes up. This will result in broadened radiation patterns due to the slight displacement of single-lobed far-field pattern of each higher order lateral mode from that of the fundamental as noted in figure. However, Qdash shows the largest degree of deterioration in divergence (FWHM of 3.4° to 10.8°) with injection due to its unique property of self-assembled highly inhomogeneous broadening gain medium that tends to result in multimode oscillation [7].

Nevertheless, Qdash shows smaller beam divergence angle than QW (FWHM ~13º) regardless of the injection. In the QW laser, filamentation is present already at near threshold injection. With increasing output power, filamentation increases with more sharp peaks appearing in the beam profile. Side lobes start to emerge at higher drive current of ~4 x

J_{th}. This nearly twin-lobed far-field profile is evidence of a curved wavefront, which is a typical feature of gain-guided devices [31]. On the other hand, intrinsic filamentation suppression in Qdot lasers contributes to small divergence angle as compared to QW and Qdash lasers. Carriers injected into the Qdots are confined by lateral energy barriers as Qdots are disconnected laterally and are cladded by higher-bandgap materials [32]. Since Qdash is formed by elongated dots and our waveguide direction is perpendicular to the dash, the optical beam divergence of the Qdash is expected to be similar to that of the QW laser while reduced filamentation characteristics of Qdot will incur in Qdash. This can be evident by the observation of the substantial improvement in the far field distributions of Qdash laser [Figure 4(b)] as compared to the asymmetric far-field pattern of QW laser [Figure 4(a)] with side lobes appearing even at low powers.

4. CONCLUSION

In conclusion, laser emission from multiple groups of Qdash ensembles in addition to multiple orders of subband energy levels within a single Qdash ensemble has been experimentally demonstrated. The suppression of laser emission in short wavelength and the progressive red-shift of longer wavelength emission with injection from short cavity length devices indicate the occurrence of photon reabsorption or energy exchange among different sizes of Qdash ensembles. These results lead to the observation of the wavelength tuned quasi-supercontinuum interband laser diodes utilizing the process of IFVD to promote group-III intermixing in InAs/InAlGaAs quantum-dash structure at an intermediate stage of intermixing. Our results show that monolithically integration of different gain sections with different bandgaps for ultra-broadband laser is feasible via the intermixing technique. In addition, Qdash laser shows similar beam divergence at high injection but improvement in filamentation as compared to QW laser due to the nature of lateral carrier diffusion, which leads to the issue of self-focusing and thus the different degrees of filamentation. However, the largest degree of broadening radiation pattern with increasing injection in Qdash structure followed by Qdot and QW in sequence indicates that improvement of inhomogeneity self-assembled active gain medium is needed especially for applications in free space communication.

ACKNOWLEDGEMENT

This work is supported by National Science Foundation (Grant No. 0725647), US Army Research Laboratory, Commonwealth of Pennsylvania, Department of Community and Economic Development. Authors also acknowledge IQE Inc. for the growth of Qdash material.

REFERENCES

[1] D. Bimberg, N. Kirstaedter, N. N. Ledenstov, Zh. I. Alferov, P. S. Kop'ev, and V. M. Ustinov, "InGaAs-GaAs quantum-dot lasers," IEEE J. Sel. Top. Quantum Electron. 3, 196-205, (1997).

[2] F. Lelarge, B. Dagens, J. Renaudier, R. Brenot, A. Accard, F. V. Dijk, D. Make, O. L. Gouezigou, J. –G. Provost, F. Poingt, J. Landreau, O. Drisse, E. Derouin, B. Rousseau, F. Pommereau, and G. –H. Duan, "Recent advances on InAs/InP quantum dash based semiconductor lasers and optical amplifiers operating at 1.55 μm," IEEE J. Sel. Top. Quantum Electron. 13, 111-124, (2007).

[3] R. H. Wang, A. Stintz, P. M. Varangis, T. C. Newell, H. Li, K. J. Malloy, and L. F. Lester, "Room-temperature operation of InAs quantum-dash lasers on InP (001)," IEEE Photon. Technol. Lett. 13, 767-769, (2001).

[4] L. Harris, D. J. Mowbray, M. S. Skolnick, M. Hopkinson, and G. Hill, "Emission spectra and mode structure of InAs/GaAs self-organized quantum dot lasers," Appl. Phys. Lett. 73, 969-971, (1998).

[5] H. Shoji, Y. Nakata, K. Mukai , Y. Sugiyama, M. Sugawara, N. Yokoyama, and H. Ishikawa, "Lasing characteristics of self-formed quantum-dot lasers with multistacked dot layer", IEEE J. Sel. Top. Quantum Electron. 3, 188-195, (1997).

[6] H. Jiang and J. Singh, "Nonequilibrium distribution in quantum dots lasers and influence on laser spectral output," J. Appl. Phys. 85, 7438-7442, (1999).

[7] H. S. Djie, B. S. Ooi, X. M. Fang, Y. Wu, J. M. Fastenau, W. K. Liu, and M. Hopkinson, "Room-temperature broadband emission of an InGaAs/GaAs quantum dots laser," Opt. Lett. 32, 44-46, (2007).

[8] A. Kovsh, I. Krestnikov, D. Livshits, S. Mikhrin, J. Weimert, and A. Zhukov, "Quantum dot laser with 75 nm broad spectrum of emission," Opt. Lett. 32, 793-795, (2007).

[9] C. L. Tan, Y. Wang, H. S. Djie, and B. S. Ooi, "Role of optical gain broadening in the broadband semiconductor quantum-dot laser," Appl. Phys. Lett. 91, 061117 1-3, (2007).
[10] B. S. Ooi, H. S. Djie, Y. Wang, C. L. Tan, J. C. M. Hwang, X. –M. Fang, J. M. Fastenau, A. W. K. Liu, G. T. Dang, and W. H. Chang, "Quantum dashes on InP substrate for broadband emitter applications", IEEE J. Sel. Top. Quantum Electron. 14, 1230-1238, (2008).
[11] H. S. Djie, C. L. Tan, B. S. Ooi, J. C. M. Hwang, X. -M. Fang, Y. Wu, J. M. Fastenau, W. K. Liu, G. T. Dang, and W. H. Chang, "Ultrabroad stimulated emission from quantum-dash laser", Appl. Phys. Lett. 91, 111116 1-3, (2007).
[12] C. L. Tan, H. S. Djie, Y. Wang, C. E. Dimas, V. Hongpinyo, Y. H. Ding, and B. S. Ooi, "Wavelength tuning and emission width widening of ultrabroad quantum dash interband laser," Appl. Phys. Lett. 93, 111101 1-3, (2008).
[13] C. Xing and E. A. Avrutin, "Multimode spectra and active mode locking potential of quantum dot lasers", J. Appl. Phys. 97, 104301 1-9, (2005).
[14] D. Garbuzov, I. Kudryashov, and M. Dubinskii, "110 W (0.9 J) pulsed power from resonantly diode-laser-pumped 1.6-μm Er:YAG laser," Appl. Phys. Lett. 87, 121101 1-3, (2005).
[15] J. R. O'Callaghan, J. Houlihan, V. Voignier, G. Huyet, J. G. McInerney, B. Corbett, and P. A. O'Brien, " Focusing properties of high brightness gain tailored broad-area semiconductor lasers", IEEE Photon. Technol. Lett. 14, 9-11, (2002).
[16] J. R. Marciante and Govind P. Agrawal, "Nonlinear mechanisms of filamentation in broad-area semiconductor lasers," IEEE J. Quantum Electron. 32, 590-596, (1996).
[17] S. Schneider, P. Borri, W. Langbein, U. Woggon, R. L. Sellin, D. Ouyang, and D. Bimberg, "Linewidth Enhancement Factor in InGaAs Quantum-Dot Amplifiers," IEEE J. Quantum Electron. 40, 1423-1429, (2004).
[18] K. Kikuchi, M. Amano, C. E. Zah and T. P. Lee, "Measurement of Differential Gain and Linewidth Enhancement Factor of 1.5-pm Strained Quantum-Well Active Layers," IEEE J. Quantum Electron. 30, 571-573, (1994).
[19] Y. Wang, H. S. Djie, and B. S. Ooi, "Group-III intermixing in InAs/InGaAlAs quantum dots-in-well," Appl. Phys. Lett. 88, 111110 1-3, (2006).
[20] H. S. Djie, Y. Wang, B. S. Ooi, D. N. Wang, J. C. M. Hwang, G. T. Dang, W. H. Chang, "Defect annealing of InAs-InAlGaAs quantum-dash-in-asymmetric-well laser," IEEE Photon. Technol. Lett. 18, 2329-2331, (2006).
[21] D. R. Matthews, H. D. Summers, P. M. Smowton, and M. Hopkinson, "Experimental investigation of the effect of wetting-layer states on the gain-current characteristic of quantum-dot lasers," Appl. Phys. Lett. 81, 4904-4906, (2002).
[22] M. van der Poel, J. Mork, A. Somers, A. Forchel, J. P. Reithmaier, G. Eisenstein, "Ultrafast gain and index dynamics of quantum dash structures emitting at 1.55 μm," Appl. Phys. Lett. 89, 081102 1-3, (2006).
[23] B. S. Ooi, K. McIlvaney, M. W. Street, A. S. Helmy, S. G. Ayling, A. C. Bryce, J. H. Marsh, and J. S. Roberts, "Selective quantum-well intermixing in GaAs-AlGaAs structures using impurity-free vacancy diffusion," IEEE J. Quantum Electron. 33, 1784-1793, (1997).
[24] H. S. Djie, Y. Wang, Y. -H. Ding, D. –N. Wang, J. C. M. Hwang, X. –M. Fang, Y. Wu, J. Fastenau, A. W. K. Liu, G. T. Dang, W. H. Chang, and B. S. Ooi, "Quantum dash intermixing," IEEE J. Sel. Top. In Quantum Electron. 14, 1239-1249, (2008).
[25] D. Hadass, R. Alizon, H. Dery, V. Mikhelashvili, G. Eisenstein, R. Schwertberger, A. Somers, J. P. Reithmaier, A. Forchel, M. Calligaro, S. Bansropun, and M. Krakowski, "Spectrally resolved dynamics of inhomogeneously broadened gain in InAs/InP 1550 nm quantum-dash lasers," Appl. Phys. Lett. 85, 5505-5507, (2004).
[26] J. H. Wei, K. S. Chan, "A theoretical analysis of quantum dash structures," J. Appl. Phys. 97, 123524 1-12, (2005).
[27] A. Markus, J. X. Chen, C. Paranthoen, A. Fiore, C. Platz, and O. Gauthier-Lafaye, "Simultaneous two-state lasing in quantum-dot lasers," Appl. Phys. Lett. 82, 1818-1820, (2003).
[28] A. Markus, M. Rossetti, V. Calligari, D. Chek-Al-Kar, J. X. Chen, A. Fiore, and R. Scollo, "Two-state switching and dynamics in quantum dot two-section lasers," J. Appl. Phys. 100, 113104 1-5, (2006).
[29] J. R. O. Callaghan, J. Houlihan, V. Voignier, G. H. Wu, E. O'Neill, J. G. Mclnerney, G. Huyet, "Spatial coherence and thermal lensing in broad-area semiconductor lasers," IEEE J. Quantum Electron. 40, 1-9, (2004).
[30] Kuo Liang and S. Wang," Spatial hole burning problems in evanescently coupled semiconductor laser arrays," Appl. Phys. Lett. 47, 555-557, (1985).
[31] J. R. Marciante and G. P. Agrawal," Controlling filamentation in broad-area semiconductor lasers," Appl. Phys. Lett. 69, 593-595, (1985).
[32] Ch. Ribbat, R. L. Sellin, I. Kaiander, F. Hopfer, N. N. Ledentsov, D. Bimberg, A. R. Kovsh, V. M. Ustinov, A. E. Zhukov, and M. V. Maximov," Complete suppression of filamentation and superior beam quality," Appl. Phys. Lett. 82, 952-954, (2003).